RESEARCH ARTICLE

WILEY Molecular Carcinogenesis

S100A11 promotes cell proliferation via P38/MAPK signaling pathway in intrahepatic cholangiocarcinoma

Mei-xia Zhang[1,2] (iD) | Wei Gan[1,2] | Chu-yu Jing[1,2] | Su-su Zheng[1,2] | Yong Yi[1,2] | Juan Zhang[1,2] | Xin Xu[1,2] | Jia-jia Lin[1,2] | Bo-heng Zhang[1,3] | Shuang-jian Qiu[1,2]

[1] The Liver Cancer Institute, Zhongshan Hospital and Shanghai Medical School, Fudan University, Shanghai, P.R. China

[2] Key Laboratory for Carcinogenesis and Cancer Invasion, The Chinese Ministry of Education, Shanghai, P.R. China

[3] Center for Evidence-Based Medicine, Fudan University, Shanghai, P.R. China

Correspondence
Bo-heng Zhang and Shuang-jian Qiu, The Liver Cancer Institute, Zhongshan Hospital and Shanghai Medical School, Fudan University, 136 Yi Xue Yuan Road, Shanghai 200032, P.R. China.
Email: zhang.boheng@zs-hospital.sh.cn (B.H.Z.); qiu.shuangjian@zs-hospital.sh.cn (S.J.Q.)

S100A11 is reported to associate with progression and poor prognosis in several tumors. We previously reported that S100A11 was highly expressed in intrahepatic cholangiocarcinoma (ICC) cells and promoted TGF-β1-induced EMT through SMAD2/3 signaling pathway. Here, we explored the prognostic role of S100A11 on ICC patients and preliminary molecular mechanisms how S100A11 regulated ICC cell proliferation. Our results showed that S100A11 was obviously increased in ICC tumor tissues. High expression of S100A11 was closely correlated with lymph node metastasis (LNM) and TNM stage and was an independent risk factor for patients' overall survival (OS) and recurrence-free survival (RFS). The nomograms comprising LNM and S100A11 achieved better predictive accuracy compared with TNM staging system for OS and RFS prediction. Silencing S100A11 significantly suppressed RBE cells and HCCC9810 cells proliferation, colony formation, and activation of P38/mitogen-activated protein kinase (MAPK) signaling pathway in vitro and inhibited tumor growth in vivo. In contrast, the overexpression of S100A11 in RBE cells and HCCC9810 cells achieved the opposite results. S100A11-induced proliferation was abolished after treatment with P38 inhibitor. Our findings suggest S100A11/P38/MAPK signaling pathway may be a potential therapeutic target for ICC patients.

KEYWORDS
intrahepatic cholangiocarcinoma, P38/MAPK, prognosis, proliferation, S100A11

1 | INTRODUCTION

Intrahepatic cholangiocarcinoma (ICC) is a rare and highly malignant liver tumor with poor prognosis.[1–4] The incidence of ICC has showed a dramatic global increasing in the last two decades, but the 5-year survival rate is less than 10%.[5] Treatment options for ICC remain unsatisfactory, early surgical resection is still only possible curative therapeutic method.[6] Unfortunately, most ICC patients are not sensitive to chemotherapy and radiotherapy.[6] Hence, it is imperative to find out novel molecular markers which can predict ICC in the early.

S100A11, also known as S100C, is a less well-known member of the S100 family.[7] Emerging evidence has revealed S100A11 serves a role in several biological processes such as cell cycle regulation, differentiation, and metastasis.[8] Increased S100A11 expression is positively related with cell metastasis, proliferation, and malignant prognosis, such as thyroid cancer, ovarian cancer,[7] lung cancer.[9]

Our previous research found that S100A11 was significantly raised in ICC cells and promoted TGF-β1-induced EMT through SMAD2/3 signaling pathway.[10,11] In present research, we aimed to explore the prognostic role of S100A11 on ICC patients and preliminary mechanisms how S100A11 regulated ICC cell proliferation were also investigated.

2 | MATERIALS AND METHODS

2.1 | Tissue samples and clinical data collection

A total of 102 ICC patients with curative resection were enrolled in this study and all from the Liver Cancer Institute, Zhongshan Hospital, Fudan University. Patients underwent regular resection (segmental resection or lobectomy) or irregular hepatectomy according to the location and size of the tumors. Twenty-five cases were treated with left hepatectomy, 19 cases with right hepatectomy, 10 cases with enlarged left hepatectomy, 13 cases with right posterior lobe, 8 cases with middle hepatectomy, 14 cases with partial right hepatectomy, and 13 cases of caudate lobe resection. There were 43 patients underwent regional lymph node dissection, seven patients among them had multi-regional lymph node dissections. Fifteen cases were treated with hepatic hilar lymph node dissection (average of three 1.8 cm metastatic lymph nodes per patient), 7 cases with posterior pancreatic lymph node dissection (average of two 2.1 cm metastatic lymph nodes per patient), 6 cases with the great omentum lymph node dissection (average of two 0.8 cm metastatic lymph nodes per patient), 11 cases with hepatic duodenal ligament lymph node dissection (average of three 1.3 cm metastatic lymph nodes per patient), 13 cases with hepatic para-aortic lymph nodes dissection (average of three 1.5 cm metastatic lymph nodes per patient). The research was approved by Zhongshan Hospital Research Ethics Committee and informed consent was obtained from each patient before specimen collection. ICC tissue specimens were confirmed by pathological diagnosis and no preoperative therapy was provided to each patient. The interval between surgery and death was defined as overall survival (OS) and interval between surgery and recurrence was defined as recurrence-free survival (RFS). The inclusion, exclusion criteria, and follow-up procedures conducted in this study were depended on our previous report.[12]

2.2 | Tissue microarray construction and immunohistochemistry

Tissue microarrays (TMAs) were constructed according to the previous literature report.[13] Two experienced pathologists helped to review ICC samples. Each case was extracted two cores (3-mm-diameter each) represented the intratumor and peritumor margin.

Monoclonal rabbit antihuman S100A11, P38, and P-P38 were purchased from abcam (Cambridge, England). Immunohistochemistry (IHC) were performed as the described.[14] The protein expression was evaluated by semiquantitative scoring system.[15] The final score was made by the positively stained tumor cells (0, no positive tumor cells; 1, <10%; 2, 10-35%; 3, 35-75%; 4, >75%) multiplied by staining intensity (1, no staining; 2, weak; 3, moderate; 4, strong). Eventually, total scores ≥ 8 were defined as high expression and those <8 were defined as low expression.

2.3 | Cell lines and main reagents

The human cholangiocarcinoma cell lines RBE (minimally metastatic), HCCC9810 (minimally metastatic) were obtained from the Chinese Scientific Academy. Three pairs of siRNAs targeting S100A11 were synthesized chemically by Biotend (Shanghai, China). The nucleotide sequence of S100A11-siRNA was shown in Table 1. Scrambled nonspecific siRNA was designed as a negative control group (Biotend). The S100A11 over-expression vector pcDNA3.1 (+) and the control vector pcDNA3.1 (−) were designed and synthesized chemically by Biotend.

2.4 | Cell culture and transfection

Cells were digested and seeded to a six-well plate at a density of 1×10^5/well. When grows to 60%, siRNA (50 nM) or 4 μg of plasmid per well with Lipofectamine 2000 (Invitrogen, Carlsbad, CA) were transfected into cells according to manufacturer's protocol. After 48 h, the efficiency of transfection was tested by western blot.

2.5 | Establishment of stable shRNA transfection

An S100A11 short hairpin (shRNA) vector was synthesized by Biotend. An shNC vector was used as a negative control. RBE cells and HCCC9810 cells were cloned into the lentiviral vector (Genechem,

TABLE 1 Sequences of three siRNAs

siRN sequence number	Nucleotide sequence (5′-3′)
S100A11-siRNA-1	
Sense	CUUCAUGAAUACAGAAUUAdTdT
Anti-sense	UAGUUCUGUAUUCAUGAAGdTdT
S100A11-siRNA-2	
Sense	GGUUAUAACUACACUCUCUdTdT
Anti-sense	AGAGAGUGUAGUUAUAACCdTdT
S100A11-siRNA-3	
Sense	CACCUGCCAAUAGUAAUAAdTdT
Anti-sense	UUAUUACUAUUGGCAGGUGdTdT

Shanghai, China). Forty-eight hours after infection, cells were selected with puromycin (6 μg/mL) for about 2 weeks to generate stable shNC and shS100A11 cells.

2.6 | Western blot

Thirty micrograms of protein was separated by 15% SDS-PAGE electrophoresis, then transferred to polyvinylidene fluoride (Millipore, Billerica, MA), and the membranes were blocked in 5% bovine serum albumin (BSA) for 1 h, then incubated with primary antibodies S100A11, P38, and P-P38 (1:1000 dilution) at 4°C. β-actin (Kangcheng, Shanghai, China) was used as an internal control. After 12 h, the membranes were incubated with secondary antibody (Kangcheng) for 1 h at room temperature. Finally, the protein bands were detected by enhanced chemiluminescent (ECL) substrate and processed by Image Lab software (Bio-Rad, Ontario, Canada).

2.7 | Cell proliferation assay

Cells were added to 96-well culture plate at a density of 3×10^3 cells/well. Cell Counting Kit-8 (CCK8) (Dojindo, Japan) was adopted to test short-term proliferation activity. After transfection every 24 h (0, 24, 48, 72, 96), 10 μL CCK8 reagent was added to each well and incubated for another 2 h. Eventually, the cells was measured at 450 nm absorbance.

2.8 | Colony-forming assay

After transfection for 24 h, cells were digested and each six-well plate was seeded 200 cells, then incubation in 37°C with 5% CO_2 for 2 weeks. When there were macroscopic colonies containing more than 50 cells, cells were washed with PBS, fixed in paraformaldehyde solution for 30 min, and dyed with giemsa for 20 min. Finally, light microscope was performed to get the image of each well.

2.9 | Flow cytometry assay

For cell cycle assay, cells were fixed in 70% alcohol at −20°C overnight after silencing 48 h, 0.5 mL PI staining binding buffer reagent (Becton Dickinson, Franklin Lakes, NJ) was added into cell suspension and incubated for 15 min at room temperature in dark. Then detected by FACSCalibur flow cytometer (Becton Dickinson).

2.10 | Tumor xenograft assay

A total of 200 μL (1×10^7 cells/mL) stable S100A11 knockdown RBE cells suspension was injected into BALB/c male nude mice (4- to 6-week-old). ShNC cells were inoculated subcutaneously on the left side and shS100A11 cells on the right side. After 30 days of injection, mice were sacrificed and tumors were taken out to be weighed and photographed. Tumor specimens were fixed in formalin and embedded in paraffin and immunohistochemical staining was adopted to detect expression of S100A11 and P-P38.

2.11 | Statistical analysis

SPSS 20.0 was used to analysis the data, the differences between groups were analyzed by one-way analysis of variance or Student's t-test. The

association between S100A11 expression and clinicopathologic characteristics was analyzed by chi-square test or Fisher's exact test. Survival rates were evaluated by Kaplan-Meier method and compared by the log-rank test. The cox proportional hazards model were adopted for univariate and multivariate analyses, variables significant on univariate analysis (defined as $P < 0.05$) were chosen as explanatory variables for the multivariate model. Data are representative of at least three

TABLE 2 Correlations between S100A11 and clinical parameters in 102 ICC patients

Parameters	Total	High	Low	P
Age (year)				
≤61	53	35	18	
>61	49	33	16	0.889
Sex				
Female	38	29	9	
Male	64	39	25	0.11
Liver cirrhosis				
Yes	17	10	7	
No	85	58	27	0.452
Tumor encapsulation				
Complete	12	6	6	
None	90	62	28	0.192
Tumor differentiation				
Well to moderately	44	30	14	
Poorly	58	38	20	0.777
Tumor number				
Single	79	55	24	
Multiple	23	13	10	0.241
Tumor size (cm)				
<5 cm	41	30	11	
≥5 cm	61	38	23	0.253
Vascular invasion				
Yes	27	17	10	
No	75	51	24	0.634
Lymph node metastasis				
Yes	43	38	5	
No	59	30	29	**0.000**
TNM stage[a]				
I + II	39	21	18	
III + IV	63	47	16	**0.031**
Child-Pugh score (A vs B)				
A	91	61	30	
B	11	7	4	1.000*

Bold values signifies $P < 0.05$.
*Tested by Fisher's exact test.
[a]According to the AJCC 7th edition TNM staging system.

experiments and are presented as means ± SD. $P < 0.05$ was considered to be statistically significant. The rms package in R project was used to establish a nomogram based on the results of multivariate analysis.[16] The predictive accuracy of the nomogram was measured by concordance index (C-index), calibration curve, and decision curve analysis (DCA) as previously described.[17] The larger the C-index, the more accurate was the prognostic prediction.[18]

3 | RESULTS

3.1 | S100A11 is highly expressed in ICC tumor tissues

A total of 102 patients were included in this study. There are 64 males and 38 females, and the average age of patients was 61.4 ± 9.7 years.

The mean tumor size was 5.4 ± 2.7 cm. Twenty-three patients carried multiple tumor nodules. Forty-three patients had lymph node metastasis (LNM). Sixty-eight out of 102 (66.7%) ICC cases had high expression of S100A11, S100A11 positively correlated with LNM and TNM stage, no significant correlation was detected with other clinical characteristics (Table 2).

We analyzed the published TCGA database and GEO datasets,[10] finding that S100A11 expression was highly expressed in several tumor tissues compared with normal tissues (Figures 1A and 1B) and significantly upregulated in ICC tissues compared with both normal (GEO/GSE 32879, $P = 0.000$) and hepatocellular carcinoma (HCC) tissues (GEO/GSE 15765, $P = 0.000$) (Figures 1C and 1D).

Then, we detected the expression of S100A11 in ICC carcinoma tissues and para-carcinoma tissues by Immunohistochemistry. As our result showed S100A11 is highly expressed
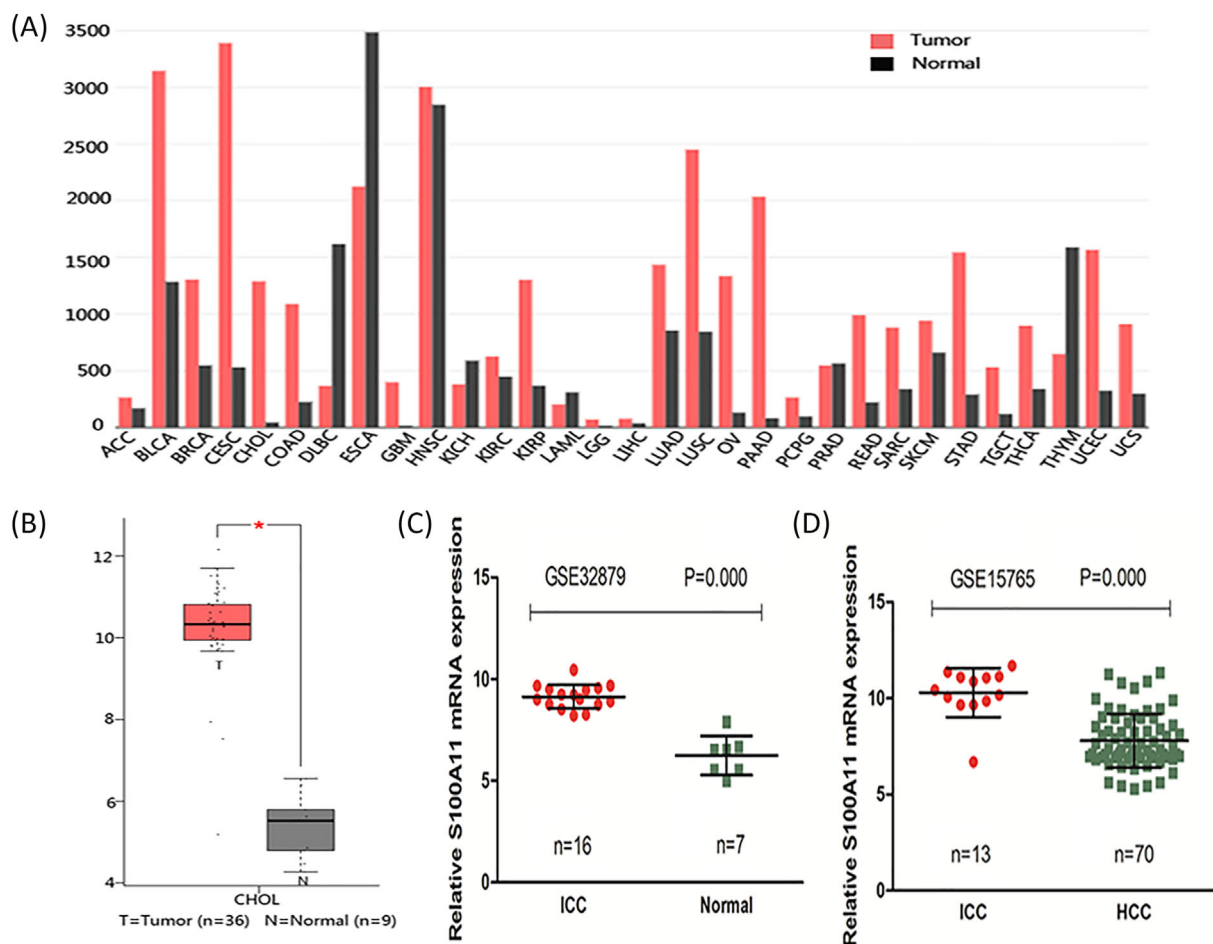

FIGURE 1   Expression of S100A11 in different tumors. A and B, Relative expression of S100A11 in several tumor tissues was higher than normal tissues and (C and D) was highly expressed in ICC tissues compared with normal and HCC tissues. *$P < 0.05$. ACC, adrenocortical carcinoma; BLCA, bladder urothelial carcinoma; BRCA, breast invasive carcinoma; CESC, cervical squamous cell carcinoma and endocervical adenocarcinoma; CHOL, cholangiocarcinoma; COAD, colon adenocarcinoma; DLBC, lymphoid neoplasm diffuse large B-cell lymphoma; ESCA, esophageal carcinoma; GBM, glioblastoma multiforme; HNSC, head and neck squamous cell carcinoma; KICH, kidney chromophobe; KIRC, kidney renal clear cell carcinoma; KIRP, kidney renal papillary cell carcinoma; LAML, acute myeloid leukemia; LGG, brain lower grade glioma; LIHC, liver hepatocellular carcinoma; LUAD, lung adenocarcinoma; LUSC, lung squamous cell carcinoma; OV, ovarian serous cystadenocarcinoma; PAAD, pancreatic adenocarcinoma; PCPG, pheochromocytoma and paraganglioma; PRAD, prostate adenocarcinoma; READ, rectum adenocarcinoma; SARC, sarcoma; SKCM, skin cutaneous melanoma; STAD, stomach adenocarcinoma; TGCT, testicular germ cell tumors; THCA, thyroid carcinoma; THYM, thymoma; UCEC, uterine corpus endometrial carcinoma; UCS, uterine carcinosarcoma

in bile duct epithelium of tumors tissues, in bile duct epithelium of para-carcinoma tissue, there is almost no S100A11 expression (Figures 2A and 2B). Representative images are shown for strong, moderate, weak, and negative expression of S100A11 in ICC tumor tissues (Figure 2C-F).

3.2 | Prognosis of S100A11 expression in ICC patients

High expression of S100A11 was positively associated with poor OS ($P < 0.001$, $\chi^2 = 13.751$) and short RFS ($P < 0.001$, $\chi^2 = 14.711$) (Figures 2G and 2H). Univariate analysis showed high expression of S100A11, tumor size, TNM stage, and LNM were unfavorable prognostic factors for OS. Unfavorable prognostic factors for RFS were S100A11 high expression, TNM stage, and LNM (Table 3). Multivariate analyses indicated that high S100A11 expression and LNM were independent prognostic factors for both OS and RFS. The S100A11-high patients were two times more likely to suffer from poorer OS and shorter RFS (Table 4).

To further investigate whether S100A11 can discriminate patients with different clinicopathologic features, subgroup analyses were performed. S100A11 was identified to stratify OS regarding tumor differentiation, tumor without lymph node metastasis (Supplementary Figure S1) and stratify RFS such as tumor without lymph node metastasis, vascular invasion (Supplementary Figure S2).
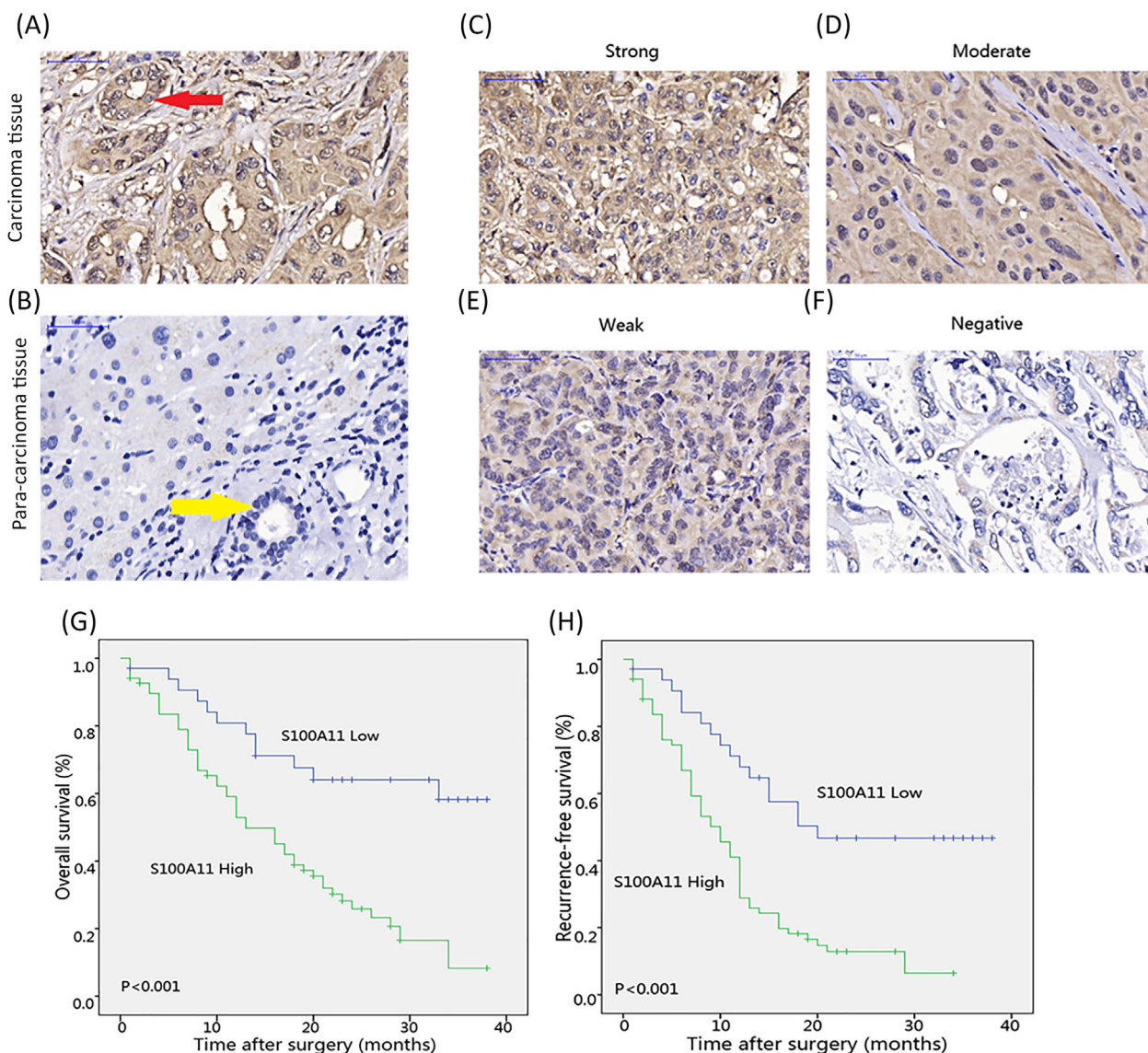

FIGURE 2 S100A11 was highly expressed in ICC tumor tissues than peritumor tissues and its clinical significance. A and B, Immunohistochemistry staining indicated expression of S100A11 is higher in bile duct epithelium of tumor tissues (red arrow), in bile duct epithelium of para-carcinoma tissue (yellow arrow), there is almost no S100A11 expression. (Magnification × 400, scale bar = 50 μm). C-F, Representative images are shown for strong, moderate, weak, and negative expression of S100A11 in ICC tumor tissues. (Magnification × 400, scale bar = 50 μm). G and H, High expression of S100A11 revealed poor OS and RFS in ICC patients

TABLE 3 Univariate analyses of factors associated with OS and RFS

	OS		RFS	
Variables	**HR (95%CI)**	**P**	**HR (95%CI)**	**P**
Age (years)	1.250 (0.758-2.601)	0.382	1.218 (0.770-1.928)	0.400
Sex	0.809 (0.488-1.342)	0.413	0.810 (0.507-1.294)	0.378
Liver cirrhosis	0.837 (0.436-1.607)	0.594	0.785 (0.430-1.431)	0.429
Tumor encapsulation	0.548 (0.219-1.366)	0.197	0.642 (0.295-1.401)	0.266
Tumor differentiation	1.241 (0.751-2.052)	0.400	1.598 (0.994-2.568)	0.053
Tumor number (multiple vs single)	1.533 (0.886-2.653)	0.126	1.419 (0.841-2.349)	0.189
Tumor size (≥5 cm vs <5 cm)	1.798 (1.054-3.068)	**0.031**	1.404 (0.87-2.266)	0.164
Vascular invasion	1.163 (0.673-2.011)	0.588	1.387 (0.841-2.288)	0.200
Lymph node metastasis	3.069 (1.840-5.120)	**0.000**	1.969 (1.241-3.124)	**0.004**
Child-Pugh score (A vs B)	1.394 (0.663-2.930)	0.381	1.324 (0.658-2.665)	0.431
TNM stage[a]	3.008 (1.675-5.402)	**0.000**	1.889 (1.152-3.097)	**0.012**
S100A11 expression (high vs low)	3.152 (1.653-6.013)	**0.000**	2.786 (1.587-4.890)	**0.000**

HR, hazard ratio; 95%CI, 95% confidence interval; OS, overall survival; RFS, recurrence-free survival. Bold values signifies $P < 0.05$.
[a]According to the AJCC 7th edition TNM staging system.

3.3 | Prognostic nomogram for OS and RFS

Nomograms are reported to have the obvious superiority compared with traditional staging system and have applied to several tumors for establishing models to predict prognosis.[19] In our research, we integrated significant independent prognostic factors (S100A11, lymph node metastasis) according to the result of multivariate analysis (Table 4) to create prognostic nomograms (Figures 3A and 3D). The C-index for OS prediction was 0.667 (95% CI, 0.663-0.671) (Figure 3A). The calibration curves reached a good consensus between OS prediction by nomogram and actual observation at 1, 2 year after surgery (Figures 3B and 3C). The prognostic nomogram for RFS is shown in Figure 3D. The C-index for RFS prediction was 0.65 (95% CI, 0.646-0.654). The calibration plot for the probability of RFS at 1, 2, 3 year after surgery showed optimal consistency between the prediction by nomogram and actual observation (Figure 3E–G).

Then, we compared the accuracy of our nomograms with the traditional TNM staging system to ascertain whether our nomograms were feasible prognostic models. Our nomograms showed better predictive accuracy (C-index, 0.667 and 0.65 for OS and RFS,

respectively) than TNM staging system (C-index, 0.598 and 0.542 for OS and RFS, respectively).

Given our nomograms suggested superior predictive capabilities compared with TNM staging system in terms of C-index, a DCA analysis was needed to compare the clinical usefulness of our constructed nomograms with TNM staging system. On DCA, nomograms demonstrated superior net benefit with wider range of threshold probability compare to TNM staging system in terms of predicting 1-, 2-year OS, and RFS (Figure 3H-K).

3.4 | S100A11 regulates cell proliferation, colony formation, and cell cycle

As our previous study demonstrated,[10] the expression of S100A11 was increased in RBE cells and HCCC9810 cells, we therefore used RBE cells and HCCC9810 cells to detect the role of S100A11 on ICC cells. Western blot result revealed S100A11 expression was dramatically reduced in RBE and HCCC9810 cells after transfected with S100A11-siRNA-2 sequence (Figure 4A-D). On the other hand, overexpression of S100A11 (S100A11) lead to a high level of

TABLE 4 Multivariate analyses of factors associated with OS and RFS

	OS		RFS	
Variables	**HR (95%CI)**	**P**	**HR (95%CI)**	**P**
Tumor size (≥5 cm vs <5 cm)	1.427 (0.813-2.506)	0.215	NA	
Lymph node metastasis	2.438 (1.039-5.719)	**0.041**	2.371 (1.158-4.856)	**0.018**
TNM stage[a]	1.143 (0.512-2.554)	0.744	1.783 (0.882-3.606)	0.107
S100A11 expression (high vs low)	2.520 (1.288-4.932)	**0.007**	2.505 (1.387-4.523)	**0.002**

HR, hazard ratio; 95%CI, 95% confidence interval; OS, overall survival; RFS, recurrence-free survival. Bold values signifies $P < 0.05$.
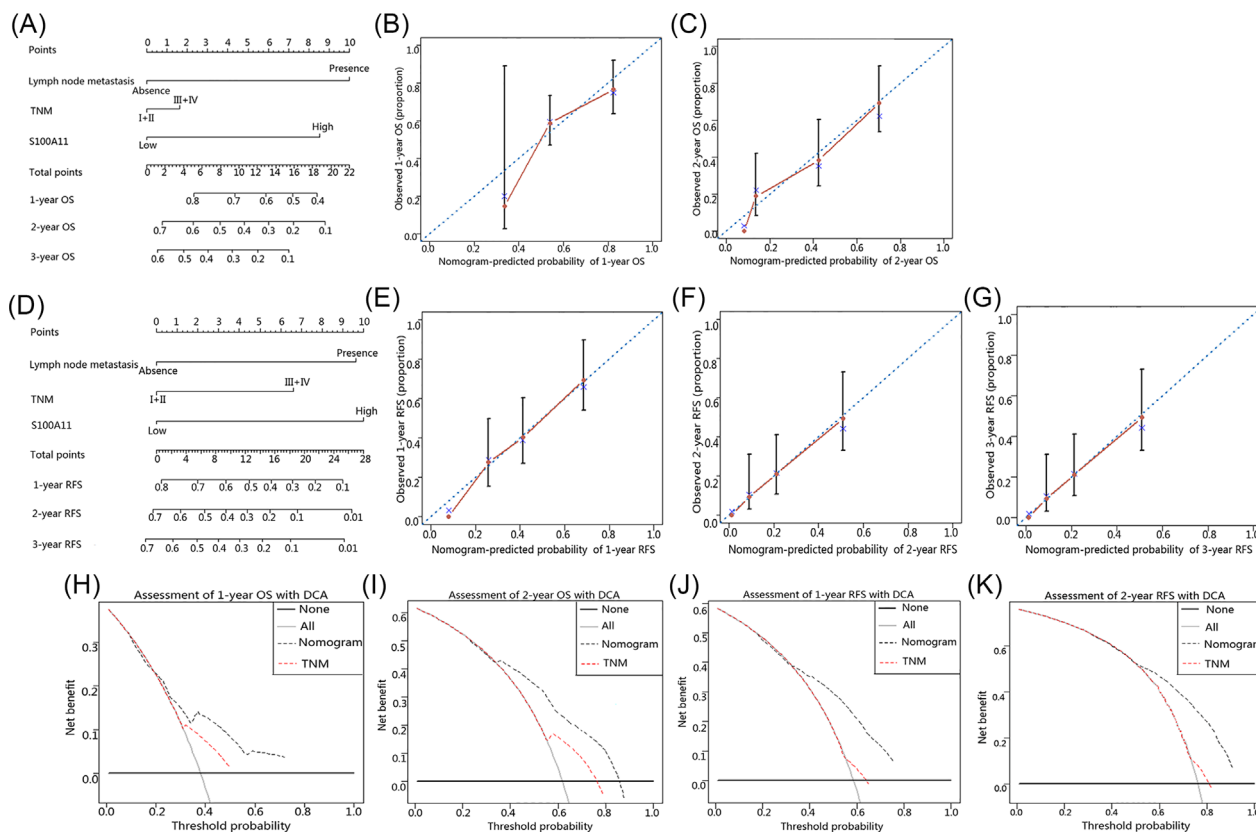[a]According to the AJCC 7th edition TNM staging system.

FIGURE 3 ICC prognostic nomogram, calibration curve, and decision curve analysis. Nomogram predicting (A) OS and (D) RFS in patients with ICC (to use the nomogram, an individual patient's value is located on each variable axis, and a line is drawn upwards to determine the number of points received for each variable value. The sum of these numbers is located on the Total Points axis, and a line is drawn downwards to the survival axes to determine the likelihood of 1-, 2-year OS, and 1-, 2-, 3-year RFS). The calibration curve for predicting OS at (B) 1 year, (C) 2 year, predicting RFS at (E) 1 year, (F) 2 year, and (G) 3 year. Nomogram-predicted probability of overall survival is plotted on the x-axis and actual overall survival is plotted on the y-axis. Decision curve analyses depict the clinical net benefit in pairwise comparisons across the different models. Nomogram is compared with the TNM stage in terms of (H) 1-year, (I) 2-year OS, and (J) 1-year, (K) 2-year RFS. Dashed lines indicate the net benefit of the predictive models across a range of threshold probabilities (black, nomogram; red, TNM stage). The horizontal solid black line represents the assumptions that no patient will experience the event, and the solid gray line represents the assumption that all patients will experience the event. On decision curve analysis, nomogram showed superior net benefit compared with TNM stage across a wider range of threshold probabilities

S100A11 compared with empty vector (vector) (Figure 4E-H). To explore the possible role of S100A11 in ICC proliferation, we used CCK8 assay to observe proliferative activity of RBE and HCCC9810 cells. As the result showed, the proliferative activity of RBE and HCCC9810 cells decreased significantly after transfected with S100A11-siRNA-2 (Figures 5A and 5C) and overexpression of S100A11 promoted the proliferation of RBE and HCCC9810 cells (Figures 5B and 5D). Consistent with cell proliferation assay, stably down-regulating S100A11 using shRNA inhibited colony formation in RBE and HCCC 9810 cells (Figure 5E-G, K-M) and colony formation increased obviously in RBE and HCCC 9810 cells after transfected with the S100A11 overexpression vector (Figure 5H-J, N-P). Cell cycle assay showed RBE cells and HCCC9810 cells were both arrested at G1 phase after knockdown of S100A11, which was consistent with other literature findings[20] (Supplementary Figure S3A-D). This result just happened to explain why proliferation was inhibited after silencing S100A11 in RBE and HCCC9810 cells.

3.5 | S100A11 regulates cells proliferation through P38/MAPK signaling pathway

Previous studies indicated that S100 family can regulate tumor proliferation and metastasis via MAPK signaling pathway.[21–24] In addition, S100A11 was reported to mediate tumor cell survival and malignant progression through activation of the P38 MAPK pathway.[25–27] Hence, we examined the levels of total P38 and its phosphorylated form (P-P38) in S100A11-silenced and S100A11-overexpressed RBE and HCCC9810 cells. As shown in Figures 6A, 6B, 6E, and 6F, silencing S100A11 dramatically reduced the P-P38 level but without significantly alter the level of total P38. In contrast, an increased level of P-P38 was observed after overexpressing S100A11 in RBE and HCCC9810 cells compared with empty vector group (Figures 6C, 6D, 6G, and 6H). In the end, an inhibitor of P38/MAPK SB203580 (10 μM, a non-cytotoxic and effective dose for blocking P38 in tumor cells) was used to block the activation of P38/MAPK
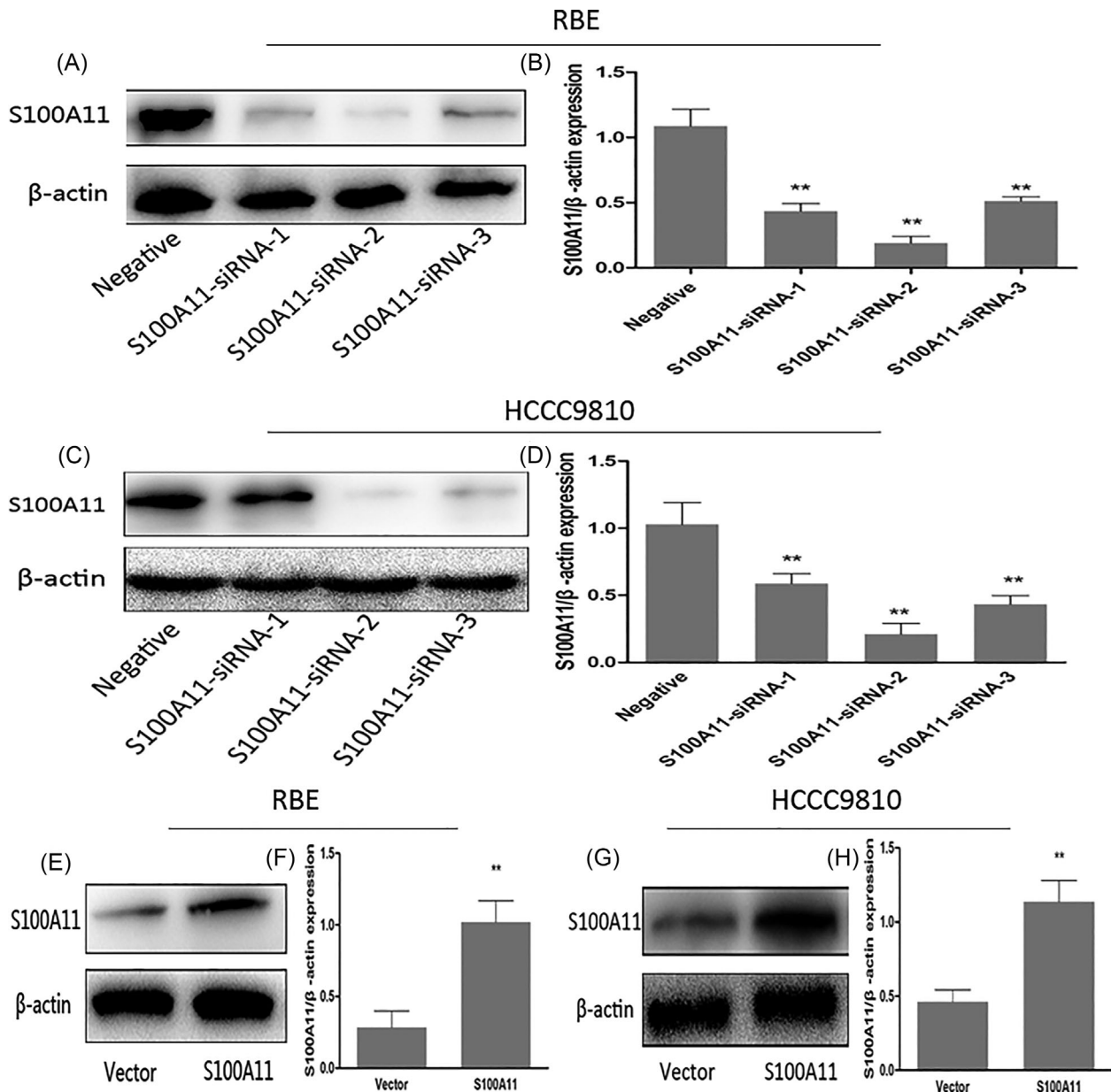
FIGURE 4 The transfection efficiency of siRNA and plasmid in RBE cells and HCCC9810 cells. A-D, Western blot revealed S100A11 expression in RBE and HCCC9810 cells was significantly lower in S100A11-si-2 group compared with negative group. E-H, Overexpression of S100A11 lead to a high level of S100A11 compared with empty vector. **$P < 0.01$

pathway in S100A11-overexpressed RBE and HCCC9810 cells, and results showed the increased proliferation induced by S100A11 overexpression vector in RBE and HCCC9810 cells were abolished after treatment with SB203580 (Figures 6I and 6J).

3.6 | Silencing S100A11 inhibits ICC xenograft tumorigenesis in vivo

As shown in Figure 7A and 7B, 30 days after RBE cells transplantation, the tumor size and weight of shS100A11 group was smaller than that of shNC group. The protein levels of S100A11 and P-P38 were significant inhibited in tumors after transfected with S100A11 shRNA (Figure 7C).

4 | DISCUSSION

Our previous work found that S100A11 was highly expressed in ICC cells and promoted TGF-β1-induced EMT through SMAD2/3 signaling pathway.[10,11] Herein, we designed this research and proved that S100A11 was highly expressed in ICC tumor tissues, predominantly stained in cytoplasm. High expression of S100A11 was positively associated with LNM and TNM stage in ICC patients, suggesting that S100A11 might be associated with poor prognosis of ICC. As literature reported, S100A11 was clinically associated with LNM and RFS[9] and LNM was also a significant prognostic factor of ICC.[28] In line with these researches, our results revealed that high expression of S100A11 was positively associated with poor OS and short RFS. Multivariate survival
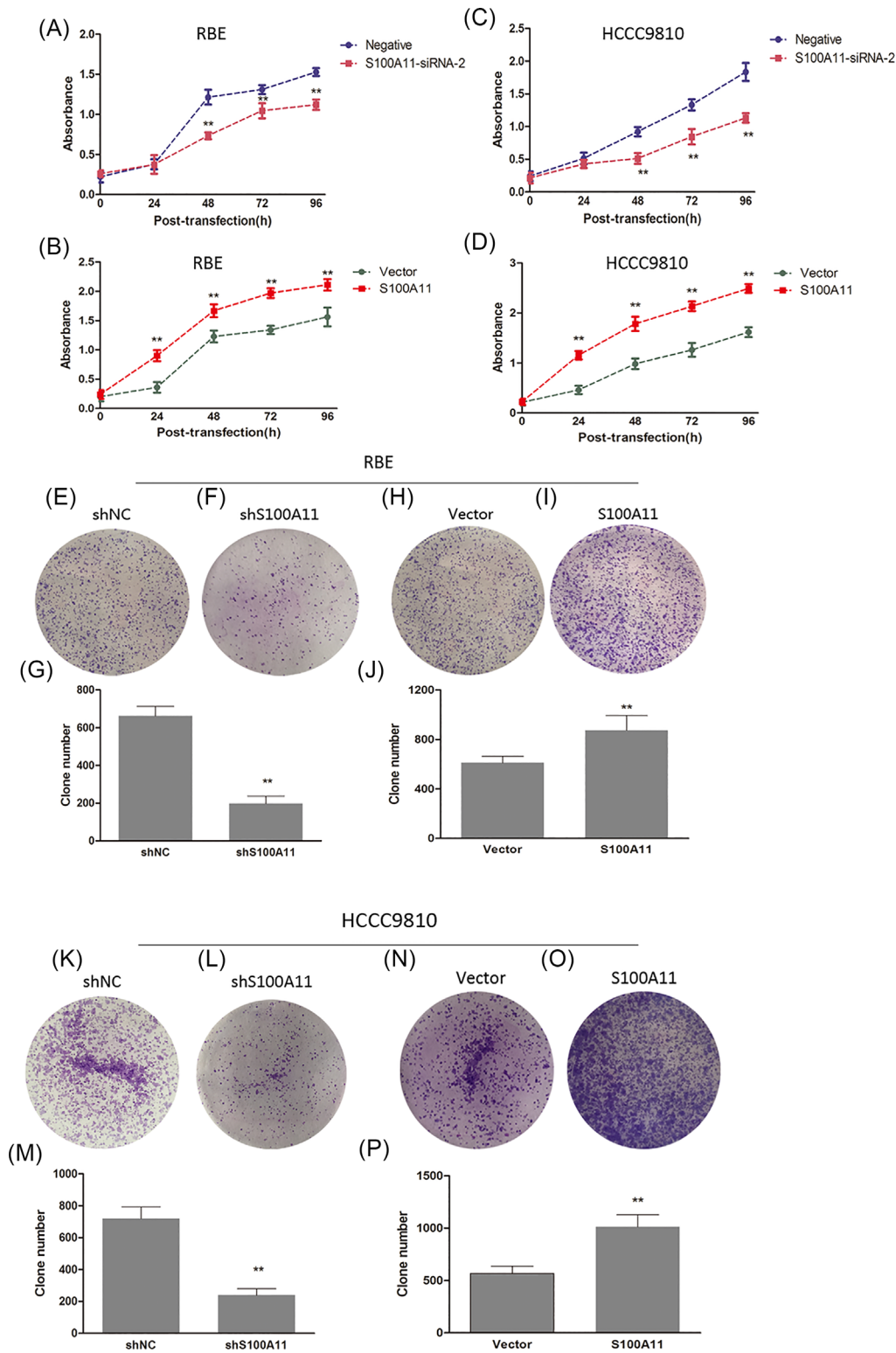
FIGURE 5 High expression of S100A11 promoted proliferation of ICC cells. A-D, CCK8 assay revealed cell proliferation was obviously decreased after transfected with S100A11-siRNA-2 and was significantly increased after overexpression of S100A11. E-P, Colony-formation assay revealed the quantity and size of the colony were significantly decreased after silencing S100A11 and increased obviously after transfected with S100A11 overexpression vector in RBE and HCCC9810 cells. **$P < 0.01$
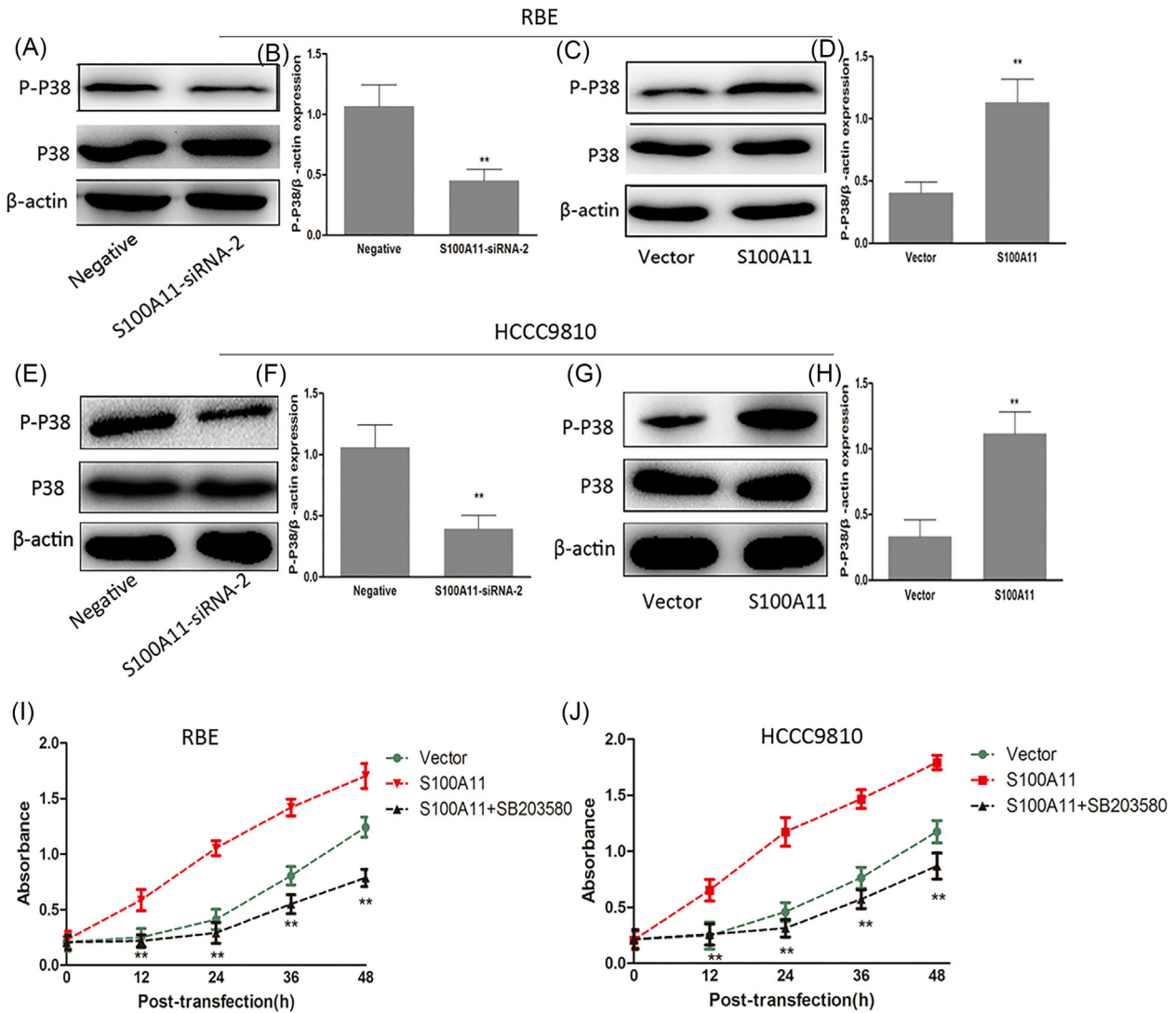
FIGURE 6 Activation of P38/MAPK signaling pathway is indispensable for S100A11 to promote the proliferation of ICC cells. A, B, E, and F, Silencing S100A11 lead to a decreased protein expression of P-P38 and (C, D, G, and H) overexpression of S100A11 increased the P-P38 level. I and J, The increased proliferation in RBE cells and HCCC9810 cells was abolished after treatment with SB203580 compared with S100A11 overexpression group. **$P < 0.01$

analysis revealed high S100A11 expression and LNM were more likely implied poorer OS and RFS. Additionally, our created nomograms integrating LNM and S100A11 expression refined better predictive accuracies in prediction of OS and RFS relative to traditional staging system TNM. These results were supportive in suggesting that S100A11 should be incorporated into ICC prognostic system to improve the discriminative ability. Collectively, our research in clinical tissues suggested that S100A11 may be a promising marker not only for distinguishing ICC from non-neoplastic disease but also for detecting the early stage of ICC and postoperative metastasis. This suggested that if ICC patients had high expression of S100A11 should be classified to be a high-risk population because of their possible poorer OS and RFS.

S100A11 deficiency has been reported to arrest cells in the G0/G1 phase[20] and inhibit TGF-β induced epithelial-to-mesenchymal transition[11,29] and suppress tumor cell proliferation.[30] In this present study, cell proliferation and colony formation were inhibited in RBE cells and

HCCC9810 cells after silencing S100A11 with siRNA or shRNA, but these effects were reversed after transfected S100A11 overexpression vector. Our results were in accordance with previous reports, which demonstrated that S100A11 promoted cell proliferation of breast cancer[31] and pancreatic carcinoma.[32] Additionally, cell cycle assay revealed cells were arrested in G1 phase in both RBE and HCC9810 cells after silencing S100A11, which was consistent with the research in renal carcinoma cells.[20] Collectively, we can draw a conclusion that cells in G1 phase are unable transit to S phase after silencing S100A11. It was just the reason the proliferative capacity of RBE and HCCC9810 cells was inhibited. Moreover, S100A11 depletion with siRNA contributed to a decreased expression of phosphorylation P38, in contrast, overexpression of S100A11 led to an increase in P-P38 level. The increase in cell proliferation by overexpression of S100A11 can be eliminated through blocking P38/MAPK signaling with SB203580. These result confirmed that activation of P38/MAPK signaling was essential for
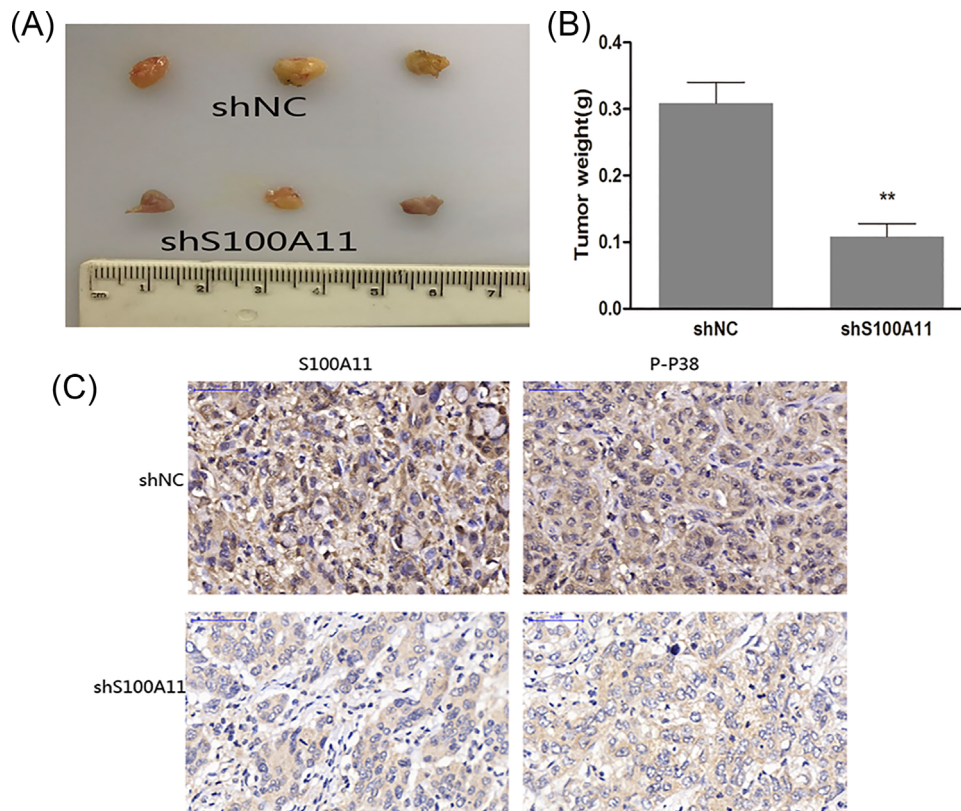
FIGURE 7 Silencing S100A11 inhibits ICC xenograft tumorigenesis in vivo. A and B, The tumor size and weight in shS100A11 group was smaller than those in shNC group. **$P < 0.01$. C, The protein levels of S100A11 and P-P38 were significant inhibited after transfected with S100A11 shRNA

S100A11 to promote proliferation of ICC cells and was consistent with other researches which indicated S100A11 accelerated inflammation and tumor malignant progression through the P38 MAPK pathway.[25-27] More importantly, the same results were proved in the in vivo experiment. The proliferation of tumors was obviously decreased and the level of S100A11 and P-P38 was significant inhibited after silencing S100A11 with shRNA in nude mice. These findings in fact verified our hypothesis that the activation of P38/MAPK signaling pathway was indispensable for S100A11 to promote ICC cells proliferation.

Several limitations to the present study should be noted. Firstly, the 102 patients collected herein were form a single institution of China. Secondly, due to our study only focused on patients underwent curative resection, whether the constructed nomograms can be applied to patients who receive non-surgical treatments remains to be explored. Thirdly, we admit it is a deficiency of our current research that the underlying mechanisms how S100A11 activate P38 in ICC is not clarified. The detailed association between S100A11 and P38 and the mechanisms how S100A11 induces P38 phosphorylation is now being explored in our next stage of cell experiment and in vivo experiment. We believe the regulatory relationship between S100A11 and P38 in ICC will be thoroughly studied in our next stage experiments.

In conclusion, despite the acknowledged limitations, the results of our clinical experiments, cell experiments in vitro, and animal experiments in vivo reached an optimal agreement: S100A11 is an independent prognostic factor of ICC and depends on the activation of P38/MAPK signaling pathway to promote ICC cells proliferation. It is worthy to consider blocking the S100A11-P38/MAPK signaling pathway combined with chemoradiotherapy to treat ICC and prevent postoperative metastasis. Further studies investigating the molecular mechanisms how S100A11 exert its multifunctional role on ICC may be a better choice for S100A11 enters into clinical application.

CONFLICTS OF INTEREST

The authors declare no conflict of interest.

ETHICAL CONDUCT OF RESEARCH

The authors state that they have followed the principles outlined in the Declaration of Helsinki for all human or animal experimental investigations. Ethical approval was obtained from the Zhongshan Hospital Research Ethics Committee, and informed consent was obtained from each patient.

ORCID

Mei-xia Zhang (iD) http://orcid.org/0000-0003-0978-4721

REFERENCES

1. DeOliveira ML, Cunningham SC, Cameron JL, et al. Cholangiocarcinoma: thirty-one-year experience with 564 patients at a single institution. *Ann Surg*. 2007;245:755–762.
2. Razumilava N, Gores GJ. *Cholangiocarcinoma Lancet*. 2014;383:2168–2179.
3. Dodson RM, Weiss MJ, Cosgrove D, et al. Intrahepatic cholangiocarcinoma: management options and emerging therapies. *J Am Coll Surg*. 2013;217:736–750 e4.
4. Poultsides GA, Zhu AX, Choti MA, Pawlik TM. Intrahepatic cholangiocarcinoma. *Surg Clin North Am*. 2010;90:817–837.
5. Fabrega-Foster K, Ghasabeh MA, Pawlik TM, Kamel IR. Multimodality imaging of intrahepatic cholangiocarcinoma. *Hepatobiliary Surg Nutr*. 2017;6:67–78.
6. Tian X, Wang Q, Li Y, et al. The expression of S100A4 protein in human intrahepatic cholangiocarcinoma: clinicopathologic significance and prognostic value. *Pathol Oncol Res*. 2015;21:195–201.
7. Liu Y, Han X, Gao B. Knockdown of S100A11 expression suppresses ovarian cancer cell growth and invasion. *Exp Ther Med*. 2015;9:1460–1464.
8. Anania MC, Miranda C, Vizioli MG, et al. S100A11 overexpression contributes to the malignant phenotype of papillary thyroid carcinoma. *J Clin Endocrinol Metab*. 2013;98:E1591–E1600.
9. Woo T, Okudela K, Mitsui H, et al. Up-regulation of S100A11 in lung adenocarcinoma—its potential relationship with cancer progression. *PLoS ONE*. 2015;10:e0142642.
10. Xue TC, Zhang BH, Ye SL, Ren ZG. Differentially expressed gene profiles of intrahepatic cholangiocarcinoma, hepatocellular carcinoma, and combined hepatocellular-cholangiocarcinoma by integrated microarray analysis. *Tumour Biol*. 2015;36:5891–5899.
11. Zhang M, Zheng S, Jing C, et al. S100A11 promotes TGF-beta1-induced epithelial-mesenchymal transition through SMAD2/3 signaling pathway in intrahepatic cholangiocarcinoma. *Future Oncol*. 2018;14:837–847.
12. Shi RY, Yang XR, Shen QJ, et al. High expression of Dickkopf-related protein 1 is related to lymphatic metastasis and indicates poor prognosis in intrahepatic cholangiocarcinoma patients after surgery. *Cancer*. 2013;119:993–1003.
13. Torhorst J, Bucher C, Kononen J, et al. Tissue microarrays for rapid linking of molecular changes to clinical endpoints. *Am J Pathol*. 2001;159:2249–2256.
14. Yang XR, Xu Y, Yu B, et al. CD24 is a novel predictor for poor prognosis of hepatocellular carcinoma after surgery. *Clin Cancer Res*. 2009;15:5518–5527.
15. Liu L, Lin C, Liang W, et al. TBL1XR1 promotes lymphangiogenesis and lymphatic metastasis in esophageal squamous cell carcinoma. *Gut*. 2015;64:26–36.
16. Wang Y, Li J, Xia Y, et al. Prognostic nomogram for intrahepatic cholangiocarcinoma after partial hepatectomy. *J Clin Oncol*. 2013;31:1188–1195.
17. Vickers AJ, Elkin EB. Decision curve analysis: a novel method for evaluating prediction models. *Med Decis Making*. 2006;26:565–574.
18. Huitzil-Melendez FD, Capanu M, O'Reilly EM, et al. Advanced hepatocellular carcinoma: which staging systems best predict prognosis? *J Clin Oncol*. 2010;28:2889–2895.
19. International Bladder Cancer Nomogram C, Bochner BH, Kattan MW, Vora KC. Postoperative nomogram predicting risk of recurrence after radical cystectomy for bladder cancer. *J Clin Oncol*. 2006;24:3967–3972.
20. Liu L, Miao L, Liu Y, et al. S100A11 regulates renal carcinoma cell proliferation, invasion, and migration via the EGFR/Akt signaling pathway and E-cadherin. *Tumour Biol*. 2017;39:1010428317705337.
21. Jin Q, Chen H, Luo A, Ding F, Liu Z. S100A14 stimulates cell proliferation and induces cell apoptosis at different concentrations via receptor for advanced glycation end products (RAGE). *PLoS ONE*. 2011;6:e19375.
22. Kwon CH, Moon HJ, Park HJ, Choi JH, Park DY. S100A8 and S100A9 promotes invasion and migration through p38 mitogen-activated protein kinase-dependent NF-kappaB activation in gastric cancer cells. *Mol Cells*. 2013;35:226–234.
23. Wu R, Duan L, Cui F, et al. S100A9 promotes human hepatocellular carcinoma cell growth and invasion through RAGE-mediated ERK1/2 and p38 MAPK pathways. *Exp Cell Res*. 2015;334:228–238.
24. Duan L, Wu R, Zou Z, et al. S100A6 stimulates proliferation and migration of colorectal carcinoma cells through activation of the MAPK pathways. *Int J Oncol*. 2014;44:781–790.
25. Sparvero LJ, Asafu-Adjei D, Kang R, et al. RAGE (Receptor for Advanced Glycation Endproducts), RAGE ligands, and their role in cancer and inflammation. *J Transl Med*. 2009;7:17.
26. Cecil DL, Johnson K, Rediske J, Lotz M, Schmidt AM, Terkeltaub R. Inflammation-induced chondrocyte hypertrophy is driven by receptor for advanced glycation end products. *J Immunol*. 2005;175:8296–8302.
27. Maletzki C, Bodammer P, Breitruck A, Kerkhoff C. S100 proteins as diagnostic and prognostic markers in colorectal and hepatocellular carcinoma. *Hepat Mon*. 2012;12:e7240.
28. Adachi T, Eguchi S. Lymph node dissection for intrahepatic cholangiocarcinoma: a critical review of the literature to date. *J Hepatobiliary Pancreat Sci*. 2014;21:162–168.
29. Niu Y, Shao Z, Wang H, et al. LASP1-S100A11 axis promotes colorectal cancer aggressiveness by modulating TGFbeta/Smad signaling. *Sci Rep*. 2016;6:26112.
30. Foertsch F, Teichmann N, Kob R, Hentschel J, Laubscher U, Melle C. S100A11 is involved in the regulation of the stability of cell cycle regulator p21(CIP1/WAF1) in human keratinocyte HaCaT cells. *FEBS J*. 2013;280:3840–3853.
31. Liu XG, Wang XP, Li WF, et al. Ca2+-binding protein S100A11: a novel diagnostic marker for breast carcinoma. *Oncol Rep*. 2010;23:1301–1308.
32. Xiao MB, Jiang F, Ni WK, et al. High expression of S100A11 in pancreatic adenocarcinoma is an unfavorable prognostic marker. *Med Oncol*. 2012;29:1886–1891.

SUPPORTING INFORMATION

Additional supporting information may be found online in the Supporting Information section at the end of the article.